

RESOLUTION OF STRUCTURE IN THE PROTOSTELLAR SOURCE IRAS 16293-2422

LEE G. MUNDY

Owens Valley Radio Observatory, California Institute of Technology

BRUCE A. WILKING

Department of Physics, University of Missouri-St. Louis

AND

STEVE T. MYERS

Owens Valley Radio Observatory, California Institute of Technology

Received 1986 September 2; accepted 1986 September 22

ABSTRACT

Emission from the cold, protostellar source IRAS 16293-2422 has been mapped in the 2.7 mm continuum and $^{13}\text{CO } J=1-0$ line with resolutions of $4'' \times 6''$ and $5'' \times 16''$, respectively. The line and continuum emission arise from a disklike structure (1800 by < 800 AU) whose major axis lies roughly perpendicular to a collimated outflow of molecular gas and the local magnetic field direction. The continuum spectrum of the dust is well fitted by a $\lambda^{-1.5 \pm 0.5}$ emissivity law and a dust temperature of 41 ± 2 K. The fits imply a total luminosity of $27 \pm 4 L_{\odot}$ and a mass of gas and dust in the range $0.9-6 M_{\odot}$. The ^{13}CO kinematics suggest that the region may be rotating.

Subject headings: infrared: sources — stars: pre-main-sequence

I. INTRODUCTION

Current models for the formation of single stars commonly include a rotating circumstellar disk of gas and dust (Pudritz 1985; Terebey, Shu, and Cassen 1984; Pudritz and Norman 1983). The disk facilitates both the infall of interstellar matter onto the forming star and the transfer of angular momentum outward. In some models, the disk also plays an important role in powering the mass outflows often associated with pre-main-sequence stars. Observationally, the ubiquity of disks, especially those envisioned by theory which extend down to the scale of hundreds of AU, is not well established. Direct evidence for such disklike structures toward a few young stellar objects has been obtained via near-infrared imaging utilizing maximum entropy image reconstruction techniques (Grasdalen *et al.* 1984; Strom *et al.* 1985), speckle interferometry (Beckwith *et al.* 1984), and observations during lunar occultation (Simon *et al.* 1985). A promising technique for the detection of disk structures and their dynamical motions has become available with the advent of millimeter-wave interferometry. Recently, thermal emission from cold dust has been detected, but not resolved, toward young embedded objects such as HL Tau (Beckwith *et al.* 1986) and L1551 IRS 5 (Keene and Masson 1986) using millimeter-wave interferometry.

This Letter reports 2.7 mm continuum and ^{13}CO spectral line observations of the young object IRAS 16293-2422 obtained with the Owens Valley (OVRO) Millimeter-Wave Interferometer. IRAS 16293-2422 is a cold, far-infrared source located in the filamentary L1689 dark cloud in the ρ Ophiuchi cloud complex. The source is identified as a deeply embedded young stellar or protostellar object based upon its coincidence with a dense clump of CS-emitting gas and a

molecular outflow (Walker *et al.* 1986a; Walker *et al.* 1986b; Wootten and Loren 1986). In addition to mass outflow, Walker *et al.* (1986a) present evidence for mass infall toward the source suggesting that it might be a true protostar yet in the stages of accretion. Our observations of IRAS 16293-2422 resolve, for the first time, the cold dust emission surrounding a pre-main-sequence star into a disklike structure of circumstellar dimensions.

II. OBSERVATIONS

Observations of the $^{13}\text{CO } J=1-0$ line and 2.7 mm continuum emission toward IRAS 16293-2422 were obtained with the OVRO three-element interferometer during the spring of 1986. The field of view of the observation was 1'1 centered at R.A.(1950) = $16^{\text{h}}29^{\text{m}}20^{\text{s}}.9$; decl.(1950) = $-24^{\circ}22'13''$. The ^{13}CO line was observed in three configurations with 50 kHz (0.14 km s^{-1}) resolution and a total bandwidth of 1.6 MHz (4.4 km s^{-1}). The filterbank was centered at $V_{\text{LSR}} = 4.0 \text{ km s}^{-1}$. The synthesized beam for these observations is $5''.3 \times 16''.2$ (position angle of 0°). The continuum emission was observed in six configurations with a 400 MHz bandwidth filter. Data from two lightly different frequencies, 110.201 GHz and 109.173 GHz, were combined to make the continuum map. The synthesized beam for the continuum observations is $3''.9 \times 6''.0$ (position angle of 0°).

The data were phase calibrated using observations of the nearby point source NRAO 530. The positional accuracy of the data is estimated to be 0.1-0.2 of a synthesized beam. The flux scale is based on observations of the planet Uranus made during each configuration. Uranus was assumed to have a flux of 12.6 Jy at 2.7 mm (Ulich 1981). The estimated uncertainty in the flux scale is 20%. While the continuum data were taken

1986ApJ...311L...75M

with either the ^{13}CO or HC_3N line in the passband, the line contamination is minimal (≤ 25 mJy) since the lines were weak.

III. RESULTS

The interferometer observations have partially resolved 2.7 mm continuum emission from IRAS 16293–2422. A map of the emission is presented in Figure 1. The observed total flux of 550 mJy arises from an elliptical region which has a half-power size of $11''$ by $< 5''$ (1800 by < 800 AU), at position angle 155° . The *IRAS* source position, shown with error bars in Figure 1, is within $2''$ of the peak of the 2.7 mm emission; there are no other *IRAS* point sources within $2'$ of that position. The continuum source lies inside of the 6500 AU infall region proposed by Walker *et al.* (1986*a*).

Our 2.7 mm continuum measurement is combined with the color-corrected *IRAS* fluxes from co-added survey data and the 1.3 mm flux (Walker *et al.* 1986*a*) in Figure 2. These data clearly define the spectral energy distribution of the source through the infrared and millimeter region. A 1 arcmin² map at $2 \mu\text{m}$ centered on the *IRAS* source position made at the IRTF revealed no detectable emission to a 3σ limit of 1.3 mJy (B. A. Wilking and E. T. Young 1985, unpublished data). Hence, the measurements from $2 \mu\text{m}$ to 2.7 mm are consistent with the continuum emission arising from cold dust. The emission is well fitted by a dust spectrum with $T_D = 41 \pm 2$ K and a λ^{-1} to λ^{-2} emissivity law. The best fit to the data occurs for a $\lambda^{-1.5}$ emissivity law which becomes optically thin longward of $400 \mu\text{m}$. The source area implied by this spectral fit is 29 arcsec^2 which is consistent with the 2.7 mm map if the unresolved minor axis is $3''.4$ in width.

The ^{13}CO $J = 1-0$ line maps show emission across the entire 4.4 km s^{-1} width of the 50 kHz filters. Through the

central channels, the emission is widely distributed over the field of view; at the ends of the filterbank, the emission arises only from the region toward IRAS 16293–2422. Figure 3 shows the ^{13}CO emission integrated from 5.63 to 6.18 km s^{-1} (*thick contours*) and from 1.82 to 2.37 km s^{-1} (*thin contours*) superposed on the half-power outline of the continuum emission. The ^{13}CO emission at these velocity extremes is clearly associated with IRAS 16293–2422. The redshifted and blueshifted emission are displaced relative to each other by $7''$ along the major axis of the continuum emission; both centroids lie within $3''$ of the continuum major axis. The position shift between the redshifted and blueshifted emission is significant at the 2σ level.

The appearance of ^{13}CO emission from IRAS 16293–2422 only at the velocity extrema may seem odd at first, but it is simply explained if the foreground portions of the ambient cloud are optically thick in the ^{13}CO line. Such large optical depth is evident toward the *IRAS* source; the ratio of the peak antenna temperatures of ^{13}CO to C^{18}O emission lines in a $1'$ beam is 2.2, well below the terrestrial optically thin ratio of 5.5 (Walker *et al.* 1986*b*). Thus, the ambient cloud ^{13}CO line, centered at 4 km s^{-1} , has sufficient optical depth around line center to absorb out the ^{13}CO emission from IRAS 16293–2422. In the line wings, the optical depth in the ambient cloud decreases to zero which allows the intrinsically wider line from the source to be seen. Since most of the gas in the ambient cloud is present in large ($> 30''$) spatial structures, the center channel maps poorly represent the true cloud column density distribution. Conversely, in the line wings, most of the ^{13}CO emission arises from the compact source whose structure is well sampled by the interferometer measurements. The optical depth in the ambient cloud makes the ^{13}CO line poorly suited for a complete kinematic analysis of

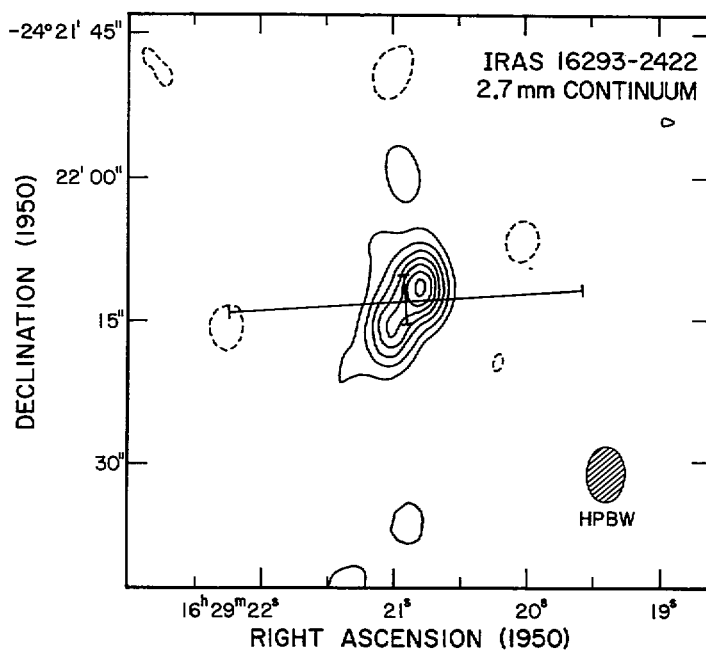


FIG. 1.—Map of the 2.7 mm continuum emission from IRAS 16293–2422. The contour levels are in steps of 40 mJy per beam from -40 (*dashed contours*) to 280 mJy. The synthesized beam half-power size ($3''.9 \times 6''.0$) is shown in the lower right-hand corner. The crossed error bars show the position and error bars for IRAS 16293–2422 given in the *IRAS Point Source Catalog* (1985).

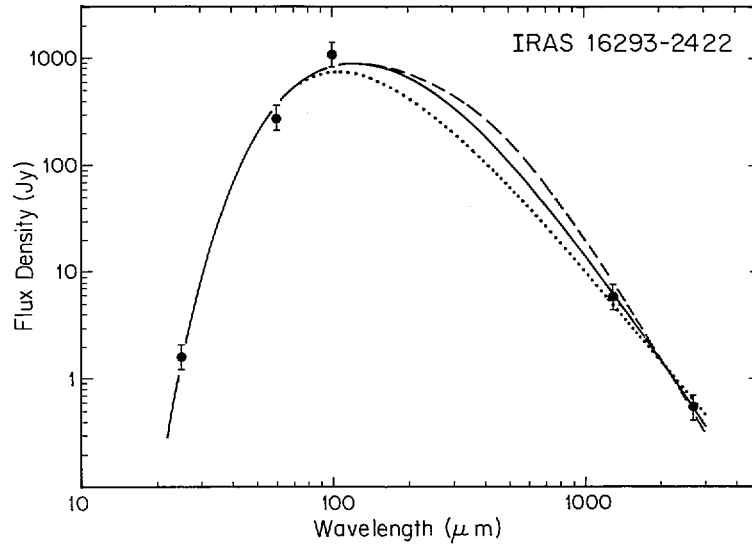


FIG. 2.—The spectral energy distribution for IRAS 16293-2422. The points with error bars show the fluxes at 25, 60, 100, and 1300 μm from Walker *et al.* (1986*a*), and at 2.7 mm from the present work. The dotted, solid, and dashed lines are fits to the data using a λ^{-1} , $\lambda^{-1.5}$, and λ^{-2} emissivity law, respectively. The dust temperature for all models is 41 K. The optical depth at 2.7 mm, source area, and luminosity are 0.060, 31 arcsec^2 , and $23 L_{\odot}$ for the λ^{-1} fit, 0.055, 29 arcsec^2 , and $27 L_{\odot}$ for the $\lambda^{-1.5}$ fit, and 0.050, 28 arcsec^2 , and $27 L_{\odot}$ for the λ^{-2} fit.

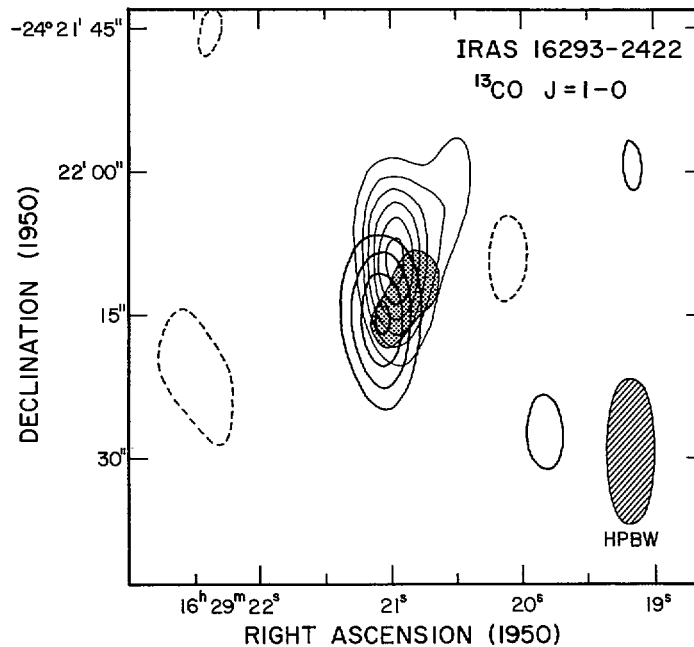


FIG. 3.—The blueshifted (*thin contours*) and redshifted (*thick contours*) $^{13}\text{CO } J=1-0$ emission toward IRAS 16293-2422 are shown superposed on the half-power outline of the continuum source. The contours are in steps of 1 Jy per beam with the lowest contours at ± 2 Jy per beam; 1 Jy per beam corresponds to 1.2 K brightness temperature. The half-power beam size ($5''.3 \times 16''.2$) is shown in the lower right-hand corner.

the velocity structure of the source; however, the spatial displacement of the velocity extrema suggests that the gas is rotating about the minor axis of the object.

IV. PHYSICAL PROPERTIES OF THE EMISSION REGION

A number of basic properties of IRAS 16293-2422 can be simply derived from the spectral energy distribution of the emission. As discussed in § III, the 25 μm –2.7 mm continuum

emission is well fitted with a 41 ± 2 K dust spectrum with a $\lambda^{-1.5 \pm 0.5}$ emissivity law. The resulting bolometric luminosity is $27 \pm 4 L_{\odot}$, assuming it is at the distance of the ρ Ophiuchi cloud complex (160 pc; Whittet 1974). The quality of the single temperature fit is unusually good in comparison to other embedded pre-main-sequence stars. For example, the mid-infrared-to-far-infrared energy distributions of objects such as S140 IRS 1 and L1551 IRS 5 are much broader than a

single temperature blackbody reflecting the presence of dust at a wide range of temperatures (Harvey, Campbell, and Hoffmann 1978; Keene and Masson 1986; Lada 1986). In the case of IRAS 16293–2422, there appears to be no detectable emission from dust warmer than 40 K. This deficiency of near-infrared emitting dust could arise because the luminosity source is so deeply embedded that even 1–10 μm photons are absorbed and degraded close to the source or because the source is intrinsically cold throughout. In either case, the $\tau = 1$ photosphere at wavelengths shortward of $\sim 100 \mu\text{m}$ corresponds to a 40 K blackbody.

The source area, as determined by our modelling, ranges from 25 to 35 arcsec^2 , depending on the choice of emissivity law. For a given emissivity, a single source size gives a good fit to the data (see Fig. 2). This is surprising given that the source area should vary with optical depth (and hence wavelength) provided the column density is not a constant across the source. For example, if the column density of an isothermal source falls off with increasing radius as r^α , then the ratio of the $\tau = 1$ source radius at two optically thick wavelengths, λ_1 and λ_2 , is given by

$$R_2/R_1 = (\lambda_2/\lambda_1)^{n/\alpha},$$

where n is the spectral index of the emissivity law. Thus, for $\alpha = 2$, the source area at 25 μm would be 4 (16) times bigger than at 100 μm for $n = 1$ (2). R_2/R_1 approaches unity only as α becomes large. Our spectral fits can, to some extent, accommodate an increasing source size with decreasing wavelength by fitting greater dust temperatures; temperature gradients within the source can also compensate for an increasing source size with decreasing wavelength. But, the fact that the minor axis of the emission is unresolved in the 2.7 mm map and that the 25 μm emission is unresolved ($< 25''$) in the in-scan direction (the direction of the small error bar in Fig. 1) in the IRAS data make it unlikely that the source size changes rapidly with wavelength. Therefore, the dust distribution in IRAS 16293–2422 is most likely very sharp-edged.

The 2.7 mm continuum flux, combined with the dust temperature determined above, can be used to derive the 2.7 mm dust optical depth, H_2 column density, A_V , and total mass of the dust and gas in the emitting region. The peak continuum emission (290 mJy per beam) corresponds to a brightness temperature of 1.2 K or a minimum optical depth of 0.033 at 2.7 mm; the actual optical depth could be larger if the synthesized beam is not filled. Assuming the dust follows a $\lambda^{-1.5}$ emissivity law and normalizing the law to $N(\text{H}_2)/\tau_{\text{dust}} = 6 \times 10^{24} \text{ cm}^{-2}$ at 400 μm (Hildebrand 1983), the peak $N(\text{H}_2)$ toward IRAS 16293–2422 is $4 \times 10^{24} \text{ cm}^{-2}$ averaged over a $4'' \times 6''$ beam. Using a standard gas-to-dust ratio (Bohlin, Savage, and Drake 1978), this corresponds to an A_V of ~ 4000 mag. Based on the integrated flux of 550 mJy, the total mass of the emitting region is 0.9, 2.3, and 6.0 M_\odot for a

λ^{-1} , $\lambda^{-1.5}$, and λ^{-2} emissivity law, respectively. Walker *et al.* (1986a) derived a somewhat smaller mass, 0.24–0.5 M_\odot for the central 1300 AU based on their infall model; given the uncertainties in both methods, the results are not inconsistent. The mass in the IRAS 16293–2422 region is much larger than the circumstellar mass derived for HL Tau, $\sim 0.01 M_\odot$ (Beckwith *et al.* 1986) but is comparable to the 0.8 M_\odot derived for L1551 IRS 5 (Keene and Masson 1986).

V. IRAS 16293–2422 AS A ROTATING DISK

There are a number of motivations for considering IRAS 16293–2422 in terms of a disk-protostar system. The asymmetry of the continuum emission, especially being unresolved along one axis, is reminiscent of an edge-on disk. The ^{13}CO emission $\pm 2 \text{ km s}^{-1}$ from line center is displaced by $7''$ along the major axis of the continuum source suggesting rotation about the minor axis. The large-scale magnetic field direction, as defined by the polarization position angles of background stars toward the periphery of the cloud (Vrba, Strom, and Strom 1976), is roughly parallel to the minor axis of the continuum emission. In addition, IRAS 16293–2422 is located in the center of a complicated outflow region where a likely outflow axis is roughly aligned with the minor axis of the continuum source (Walker *et al.* 1986b; Wootten and Loren 1986).

Our observations are consistent with both the dust and line emission arising from a rotating disk. The disk mass necessary to remain gravitationally bound with the velocity excursions seen in the ^{13}CO observations, $\pm 2 \text{ km s}^{-1}$ from line center, is 2 M_\odot which is consistent with the observed continuum emission if the wavelength dependence of the emissivity is about $\lambda^{-1.5}$ or steeper. The gravitational binding energy of such a disk is also sufficient to stabilize the structure against disruption by the stellar wind responsible for accelerating the high-velocity molecular gas (Wootten and Loren 1986). The sharp-edged nature of the source and the narrow minor axis fall in line with the thin accretion disks predicted by some models (e.g., Pudritz 1985). The luminosity of the system ($\sim 27 L_\odot$) is also in the range expected during the protostellar phase of a 0.5–1 M_\odot star (Adams and Shu 1985; Stahler 1983). One potential difficulty with the disk interpretation is that such cold, massive disks are highly unstable (cf. Larson 1984). Confirmation of the disk model hinges on the definitive measurement of the velocity structure along the major axis of the emission region and resolution of the minor axis.

We thank S. L. Scott and D. P. Woody for their assistance in the observations and R. E. Miller of A.T.T.B.L. for providing SIS junctions used in the receivers. We gratefully acknowledge fruitful discussions with Charles Lada, Chris Walker, and Erick Young. B. A. W. acknowledges a Weldon Springs award from the University of Missouri. L. G. M. and S. T. M. acknowledge support from NSF grant AST84-12473.

REFERENCES

- Adams, F. C., and Shu, F. H. 1985, *Ap. J.*, **296**, 655.
 Beckwith, S., Sargent, A. I., Scoville, N. Z., Masson, C. R., Zuckerman, B., and Phillips, T. G. 1986, *Ap. J.*, **309**, 755.
 Beckwith, S., Zuckerman, B., Skrutskie, M. F., and Dyck, H. M. 1984, *Ap. J.*, **287**, 793.
 Bohlin, R. C., Savage, B. D., and Drake, J. F. 1978, *Ap. J.*, **224**, 132.
 Grasdalen, G. L., Strom, S. E., Strom, K. M., Capps, R. W., and Thompson, D. 1984, *Ap. J. (Letters)*, **283**, L57.
 Harvey, P. M., Campbell, M. F., and Hoffmann, W. F. 1978, *Ap. J.*, **219**, 891.

- Hildebrand, R. H. 1983, *Quart. J.R.A.S.*, **24**, 267.
IRAS Point Source Catalog 1985, Joint *IRAS* Science Working Group
(Washington, D. C.: U. S. Government Printing Office).
Keene, J. B., and Masson, C. R. 1986, in preparation.
Lada, C. J. 1986, in *IAU Symposium 115, Star Forming Regions*, ed. M.
Peimbert and J. Jugaku (Dordrecht: Reidel), in press.
Larson, R. B. 1984, *M.N.R.A.S.*, **206**, 197.
Pudritz, R. E. 1985, *Ap. J.*, **293**, 216.
Pudritz, R. E., and Norman, C. A. 1983, *Ap. J.*, **274**, 677.
Simon, M., Peterson, D. M., Longmore, A. J., Storey, J. W. V., and
Tokonaga, A. T. 1985, *Ap. J.*, **298**, 328.
Stahler, S. W. 1983, *Ap. J.*, **274**, 822.
Strom, S. E., Strom, K. M., Grasdalen, G. L., Capps, R. W., and
Thompson, D. 1985, *A.J.*, **90**, 2575.
Terebey, S., Shu, F. H., and Cassen, P. 1984, *Ap. J.*, **286**, 529.
Ulich, B. L. 1981, *A.J.*, **86**, 1619.
Vrba, F. J., Strom, S. E., and Strom, K. M. 1976, *A.J.*, **81**, 958.
Walker, C. K., Lada, C. J., Young, E. T., Maloney, P. R., and Wilking,
B. A. 1986a, *Ap. J. (Letters)*, **309**, L47.
Walker, C. K., Lada, C. J., Young, E. T., Margulis, M., Maloney, P., and
Wilking, B. A. 1986b, in preparation.
Whittet, D. C. B. 1974, *M.N.R.A.S.*, **196**, 469.
Wootten, H. A., and Loren, R. B. 1986, *Ap. J.*, submitted.

LEE G. MUNDY and STEVE T. MYERS: California Institute of Technology, Mail Stop 105-24, Pasadena, CA 91125

BRUCE A. WILKING: Department of Physics, University of Missouri–St. Louis, 8001 Natural Bridge Road, St. Louis, MO 63121